Pravesh Singh, 2026, 14:4
ISSN (Online): 2348-4098
ISSN (Print): 2395-4752

International Journal of Science, Engineering and Technology
An Open Access Journal

Design and Analysis of a Multiband Fractal Antenna Using Shape, Size, Scaling Factor, and Iteration Optimization for 5G and Beyond Networks

Pravesh Singh[1], Sharad Kumar[2]

[1]Research Scholar, Department of Electronics & Communication Engineering, Shri Venkateshwara University, Gajraula India,
[2]Associate Professor, Department of Electronics & Communication Engineering, Shri Venkateshwara University, Gajraula India

Abstract- Multiband antennas must provide useful radiation across selected frequency intervals while satisfying size, fabrication, and integration constraints. Fractal geometries offer multiple geometric scales, but additional iterations do not necessarily produce wider bandwidth or higher efficiency. This paper develops a literature-informed design and analysis framework for jointly optimizing radiator shape, overall size, scaling factor, and iteration order. A printed, microstrip-fed fractal monopole is proposed as the initial platform, with Sierpinski-type, Koch-type, and conventional geometries compared under controlled substrate and ground conditions. Analytical examples quantify frequency scaling, geometric path growth, and sensitivity to dimensional and dielectric changes. A constrained multiobjective workflow is formulated to balance impedance coverage, realized gain, efficiency, and occupied area. The analysis shows that a single geometric scaling factor cannot independently place three arbitrarily selected resonance frequencies and that physical miniaturization must be evaluated using the complete antenna structure. The contribution is a reproducible design methodology and calculated feasibility assessment, rather than a validated antenna prototype. Full-wave optimization, fabrication, and measurements remain necessary before performance or network compatibility can be established.

Keywords: Fractal antenna, multiband operation, scaling factor, iteration optimization, 5G, multiobjective design.

I. INTRODUCTION

Wireless terminals increasingly require several operating bands within restricted installation volumes. Antenna development must therefore address frequency coverage, radiation efficiency, mechanical integration, and repeatability together. A radiator with several deep reflection minima may still be unsuitable if its bandwidth excludes required channels or its accepted power is dissipated. Multiband design is consequently an electromagnetic and system-integration problem, not simply the generation of multiple resonances.

Fractal antenna engineering applies repeated geometric transformations to radiating elements and arrays. The resulting structures contain different characteristic lengths and can redistribute current within a compact footprint. Werner and Ganguly (2003) distinguish the use of fractal geometry in individual radiators from its use in arrays. That distinction matters because element miniaturization and array beam control are separate design objectives. This paper concentrates on a single printed element and treats array integration as subsequent work.

For a concrete application, the framework considers separate mid-band frequency windows within 3.3–3.8 GHz and 4.4–5.0 GHz. These intervals correspond to NR bands n78 and n79 in the cited Release 18 specification (European Telecommunications Standards Institute [ETSI], 2026). They are design targets, not measured coverage. A resonance at one frequency inside either interval does not establish support for the entire band, and spectrum availability must be checked for the deployment region.

The phrase “beyond networks” describes an extension pathway rather than demonstrated 6G capability. The International Telecommunication Union (ITU, 2023) provides a framework for IMT-2030 that extends beyond antenna frequency response to broader capabilities and usage scenarios. Accordingly, a sub-6-GHz fractal element cannot establish compliance with future network requirements. The research question addressed here is narrower: how should shape, size, scaling, and iteration be optimized jointly without confusing geometric complexity with useful electromagnetic performance?

II. LITERATURE REVIEW AND DESIGN RATIONALE

Puente-Baliarda et al. (1998) investigated the Sierpinski multiband fractal antenna and connected its response to geometric self-similarity. Romeu and Soler (2001) subsequently examined generalized Sierpinski constructions. These studies support using scaled substructures to guide resonance placement, but they do not justify treating every fabricated motif as an independently matched resonator. Feed excitation, truncation, coupling, and the finite ground alter the practical response.

Koch constructions address a related but different mechanism: increasing conductor path complexity within a bounded region. Puente-Baliarda et al. (2000) analyzed the Koch monopole, providing a basis for studying compact radiators. However, physical path growth and electrical length are not interchangeable. Closely spaced segments interact, and currents with opposing directions may contribute differently to radiation than isolated straight conductors. Therefore, perimeter alone is an inadequate optimization objective.

Evidence also challenges the assumption that higher iteration necessarily improves bandwidth. Borja and Romeu (2003) examined Koch-island boundary microstrip patches and reported behavior involving quality factor and localized modes. Their work motivates explicit bandwidth and pattern evaluation rather than selection by iteration count. Although printed patches and monopoles differ, the methodological lesson is transferable: geometry changes must be evaluated through the actual current distribution and radiation response of the selected topology.

Recent work by Yaminisasi et al. (2025) combines a compact fractal monopole, partial fractal ground, and machine-learning-assisted parameter prediction. It illustrates the relevance of data-assisted design, while also highlighting the number of interacting design variables. Here, the initial ground remains simple so that changes caused by the radiator can be distinguished from changes caused by ground modification. The proposed contribution is this controlled joint-optimization protocol and its analytical feasibility checks; global novelty of the geometry is not claimed.

III. METHODOLOGY

Study Design and Evidence Boundaries

This is a conceptual engineering study combining a focused literature synthesis, closed-form calculations, and a proposed computational protocol. Foundational fractal studies were selected for their geometric mechanisms; a recent optimization study was included for methodological context; official standards establish the stated frequency intervals. This is not an exhaustive systematic review. No solver dataset, fabricated sample, measured radiation pattern, or optimizer output was available, so all design settings are explicitly provisional.

The analysis separates three evidence categories. Published findings support qualitative design rationale. Calculated quantities follow the equations and assumptions stated below. Proposed targets define future acceptance criteria and are not results. This separation prevents analytical resonance estimates from being presented as full-wave predictions. It also permits subsequent researchers to replace provisional inputs while preserving the comparison logic.

Antenna Platform and Geometric Variables

The proposed platform is a planar radiator printed above a partial rectangular ground on the opposite substrate face and excited by a nominal 50-ohm microstrip feed. It is a printed monopole, rather than a conventional cavity-backed microstrip patch. A provisional board envelope of 40 × 35 mm, substrate thickness of 1.6 mm, and relative permittivity of 4.4 define the starting model. These values are engineering assumptions, not a characterized material specification.

A baseline triangular radiator is compared with a Sierpinski-type radiator and a Koch-type boundary variant. Figure 1 illustrates the classical Sierpinski construction at successive iterations; it is a geometry explanation, not a fabrication drawing. Generalized scaling requires a separate parameterized coordinate definition. The initial radiator height is bounded between 15 and 30 mm, with width constrained to fit the board. Feed width is calculated from the actual substrate stack and then adjusted only within declared bounds.

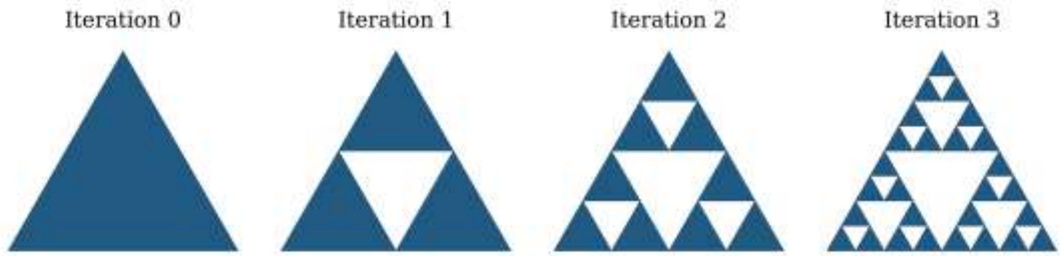

Figure 1 Classical Sierpinski Geometry Across Four Iteration Orders

Note. Original schematic with s = 0.50. Blue denotes retained planar area. Feed, substrate, and ground are omitted; the panels are not fabrication layouts. Construction context: Puente-Baliarda et al. (1998).

The main variables are shape family, global size multiplier, child-to-parent scale ratio, and integer iteration order. Feed position, feed-to-ground relationship, and trace width are nuisance variables that must also be recorded. Otherwise, attributing an improved response solely to fractal iteration would be misleading. Table 1 defines the proposed search space and clarifies which settings describe geometry and which govern feasibility.

Table 1 Provisional Design Space and Feasibility Controls

Variable	Proposed values	Purpose
Shape family	Triangle; Sierpinski-type; Koch-type	Controlled geometry comparison
Radiator height	15–30 mm	Lowest-mode tuning
Scale ratio, s	0.50–0.85	Relative mode placement
Iteration order, n	0, 1, 2, 3	Complexity screening
Board envelope	40 × 35 mm initially	Fixed-envelope baseline
Minimum trace/gap	0.30 mm	Fabrication constraint

Note. Author-proposed settings, not optimized dimensions. Scaling definitions are family-specific; geometric validity must be checked before simulation.

Two comparisons are required. A fixed-envelope comparison holds the board and ground constant to evaluate performance within the same installation space. A frequency-matched comparison retunes each candidate to the same lowest target frequency before comparing size. Removing copper while retaining the original board does not constitute a reduction in installation area. Both radiator area and complete board area should therefore be reported.

Analytical Scaling and Iteration Relations

For similar active current paths in approximately unchanged dielectric loading, a first-order resonance estimate is $f \approx c/(kL\sqrt{\varepsilon_{eff}})$, where c is free-space wave speed, L is effective path length, ε_{eff} is effective relative permittivity, and k represents the resonance topology. A quarter-wave path uses $k \approx 4$, whereas a half-wave path uses $k \approx 2$. This relation is a preliminary sizing heuristic; the proposed finite-ground monopole requires electromagnetic calibration.

$$L_n = L_0 s^n; \quad f_n/f_0 \approx s^{-n}, \quad 0 < s < 1. \quad (1)$$

Equation 1 describes ideal self-scaling with iteration index n. It predicts possible frequency ratios rather than guaranteed matched bands. For a classical Koch curve, four segments replace each original segment, each with one-third its length, so the geometric path is $P_n = P_0(4/3)^n$. For a classical Sierpinski gasket, retained area is $A_n = A_0(3/4)^n$. Neither expression predicts realized gain, impedance bandwidth, or efficiency.

For a 3.5-GHz sizing illustration with $\varepsilon_{eff} = 2.7$ and $k = 4$, the estimated active path is approximately 13.0 mm. This is not a final radiator height because fringing, feed coupling, and return currents contribute to the resonance. Uniform geometric scaling is also approximate when substrate thickness and connector size remain unchanged. Consequently, an optimization routine must distinguish scaling the radiator alone from scaling the entire electromagnetic structure.

Optimization Objectives and Constraints

The design vector x contains the discrete shape and iteration choices plus continuous dimensions. The optimization should minimize board area and worst-band mismatch while maximizing the minimum radiation efficiency over all required intervals. Realized gain and pattern coverage are retained as feasibility constraints. A Pareto approach is appropriate because smaller dimensions may worsen efficiency or narrow the matched bandwidth. NSGA-II provides an established nondominated sorting approach for exploring such trade-offs (Deb et al., 2002).

$$M(x) = \max \text{ over } f \in B \text{ of } |S_{11}(f, x)|; \quad \text{minimize } [A_{board}(x), M(x), -\eta_{min}(x)]. \quad (2)$$

Here B is the union of the required frequency intervals, not the gap between them, and η_{min} is the lowest radiation efficiency within B. The initial matching constraint is $M \leq 0.316$, equivalent to $S_{11} \leq -10$ dB. Proposed efficiency and realized-gain floors are 60% and 2 dBi, respectively, subject to a later link budget. These are study targets rather than universal 5G requirements. Gain must be evaluated in the intended service directions, not only at the peak.

Constraints also exclude disconnected copper islands unless intentionally modeled, overlapping features, insufficient feed clearance, and traces or gaps below 0.30 mm. This feature limit is provisional and must be agreed with the fabricator. A candidate satisfying nominal constraints should then undergo tolerance analysis. Robust selection should prioritize designs maintaining coverage under perturbations, rather than an isolated solution with an exceptionally deep reflection minimum.

Simulation and Experimental Validation Protocol

The computational workflow begins with identical substrate, conductor-loss, port, boundary, and ground definitions for each family. First, sweep size and feed parameters for the nonfractal reference. Second, screen iteration orders and scaling ratios. Third, refine promising candidates using joint optimization. Use a preliminary 2–6-GHz sweep to identify nearby modes, followed by dense evaluation across both required intervals. Adaptive frequency sampling should be checked using discrete solutions near narrow resonances and band edges.

Proposed convergence gates are less than 0.5% change in resonance frequency and less than 0.02 change in linear reflection magnitude between successive mesh refinements at critical frequencies. Edge and gap regions require local refinement. The final report should record solver version, element count, port reference plane, boundary clearance, and power balance. These gates are specified for reproducibility and have not been executed in this study.

For stochastic optimization, an initial budget of 40 candidates over 50 generations may be tested using five independent seeds. The budget must be reported as actual electromagnetic evaluations, including failed geometries and repeated validation. A surrogate model may reduce cost, but geometry-level holdout sets are needed to avoid placing samples from one design in both training and testing. Every selected surrogate optimum must be reevaluated in the full-wave solver.

Fabrication should include at least three independently produced copies of the selected candidate and the reference design. Reflection measurements require calibration to a stated reference plane, while chamber measurements should establish gain, efficiency, polarization, and angular coverage. Connector attachment and cable routing must be documented. Differences among copies should be reported directly; three samples offer an initial repeatability check, not strong statistical evidence of production yield.

IV. ANALYTICAL RESULTS AND DISCUSSION

Scaling Feasibility

Table 2 and Figure 2 present calculated frequency sequences for a reference frequency of 3.5 GHz using Equation 1. With s = 0.50, the next estimated frequencies are 7.0 and 14.0 GHz. Such octave spacing does not place successive resonances near 3.5 and 4.7 GHz. Increasing s to 0.75 produces approximately 4.67 and 6.22 GHz. These results demonstrate a geometric placement issue before expensive simulation, but they do not demonstrate electromagnetic operation at those frequencies.

Table 2 Calculated Resonance Sequences Under Ideal Self-Scaling

Scale ratio, s	f_0 (GHz)	f_1 (GHz)	f_2 (GHz)
0.50	3.50	7.00	14.00
0.65	3.50	5.38	8.28
0.75	3.50	4.67	6.22

Note. Calculated from $f_n = 3.5s^{-n}$. Values indicate ideal scaling only and do not establish matched bands, bandwidth, or radiation performance.

Figure 2 Idealized Frequency Scaling for Three Scale Ratios

Note. Original analytical plot from Equation 1 with f_0 = 3.5 GHz. Lines connect calculated geometric levels; no simulated or measured antenna response is represented.

A more revealing example uses hypothetical resonance targets of 3.5, 4.7, and 5.8 GHz. The required successive child-to-parent ratios are 3.5/4.7 = 0.745 and 4.7/5.8 = 0.810. Because the ratios differ, one constant scale factor cannot place all three exactly under Equation 1. A generalized construction, separate slot dimensions, or controlled coupling is needed. The 5.8-GHz value is only an analytical example and is not presented as an NR allocation.

This finding supports testing nonuniform scaling, as motivated by generalized Sierpinski designs (Romeu & Soler, 2001), while also exposing a terminology issue. A geometry with independently adjusted levels is not strictly self-similar. It should be described as generalized or fractal-inspired, with its actual coordinate-generation rule disclosed. Retaining the word "fractal" does not remove the need to explain which dimensions control each mode.

Iteration, Size, and Bandwidth Trade-offs

At Koch iterations zero through three, normalized geometric path length becomes 1.000, 1.333, 1.778, and 2.370. For the Sierpinski construction, retained area becomes 1.000, 0.750, 0.563, and 0.422. These quantities describe different families and must not be combined as the performance of one antenna. They show increasing complexity, but they contain no conductor-loss or coupling information and cannot establish an optimal iteration.

The practical stopping rule should therefore be marginal electromagnetic benefit. An additional iteration is justified only if it improves required-band coverage, reduces complete installation size, or strengthens robustness without violating radiation constraints. If it creates a narrow unused mode while increasing fabrication sensitivity, it should be rejected. This decision rule is consistent with the need to examine mode and quality-factor behavior demonstrated by Borja and Romeu (2003).

Full-band matching is demanding. Covering 3.3–3.8 GHz requires approximately 14.1% fractional bandwidth around the arithmetic center, while 4.4–5.0 GHz requires approximately 12.8%. These values follow $100(f_{high} - f_{low})/f_{center}$. A design targeting narrower regional channels may need less bandwidth, but that change must be declared before optimization. Selecting favorable intervals after observing the response would overstate the original design success.

Tolerance and Performance Interpretation

Differentiating the resonance heuristic yields $\Delta f/f \approx -\Delta L/L - 0.5\Delta\varepsilon_{eff}/\varepsilon_{eff}$. A 1% increase in effective path length gives approximately a 1% frequency decrease, or 35 MHz at 3.5 GHz. A 5% increase in effective permittivity gives approximately a 2.5% decrease, or 87.5 MHz. These independent, first-order scenarios are sensitivity illustrations, not measured tolerances or probabilities. They show why margin at required band edges matters.

Matching must also be interpreted through power. At $S_{11} = -10$ dB, reflected power is 10% and the accepted fraction is 90%. If radiation efficiency were 60%, total efficiency would be 54% under the single-port relation $\eta_{total} = \eta_{rad}(1 - |S_{11}|^2)$. The efficiency value is hypothetical. This calculation demonstrates why a satisfactory reflection coefficient alone cannot establish useful radiation or battery-efficient operation.

To isolate causation in future results, remove one modification at a time while preserving the feed and substrate: compare the plain radiator, first fractal level, second level, and generalized scaling. Repeat the comparison after allowing equal tuning effort for each candidate. Current maps at every target resonance should identify whether the active path lies on the radiator, feed, or ground. A mode dominated by the ground must not be attributed automatically to fractal self-similarity.

Implications for 5G and Beyond Integration

A successful single element would still require evaluation in its intended enclosure. Batteries, displays, cables, and neighboring antennas alter current paths and detune bands. Extension to multiple-input multiple-output operation needs embedded-element patterns, coupling, efficiency, and correlation evaluated under stated terminations. A free-space single-port result is insufficient to establish device throughput, diversity improvement, or user-loaded performance.

Frequency scaling toward millimeter-wave operation also requires a new material and integration assessment. Conductor roughness, fabrication resolution, dielectric characterization, feed losses, and packaging become relevant to the scaled implementation. Reusing the same drawing at a smaller size would not preserve all electromagnetic conditions. The credible beyond-5G contribution is a transferable optimization and validation method, aligned with the broader development perspective of ITU (2023), rather than an unsupported claim of universal network compatibility.

V. LIMITATIONS AND FUTURE RESEARCH

The principal limitation is the absence of full-wave and experimental data. No optimal shape, final dimensions, bandwidth curve, gain value, efficiency measurement, or production yield has been established. The proposed material properties, search bounds, and acceptance floors require application-specific revision. The literature review is selective, and cross-study performance rankings are deliberately avoided because substrates, grounds, measurement procedures, and frequency ranges differ.

Future work should first execute the controlled baseline comparisons and publish coordinate files, solver settings, and raw frequency responses. It should then investigate nonuniform scaling, uncertainty-aware optimization, enclosure loading, and multi-element integration. If a simpler nonfractal candidate meets the same constraints with less cost or sensitivity, that result should guide selection. The purpose of optimization is a better antenna, not confirmation that a preferred geometric family must win.

VI. CONCLUSION

Joint optimization of shape, size, scaling factor, and iteration offers a structured route to multiband printed antenna development. The analytical results establish that constant geometric scaling restricts resonance placement, increasing iteration measures complexity rather than guaranteed performance, and material or dimensional variation can consume practical band-edge margin. The proposed workflow combines controlled baselines, interval-based matching, radiation constraints, and tolerance assessment. It provides a defensible starting point for 5G-oriented design, while full-wave simulation and measurement remain essential before declaring an optimized antenna or extending performance claims to future networks.

Declarations

Data availability: All analytical inputs and calculation rules are included in this paper; no experimental dataset was generated. Funding and competing interests: Author confirmation is required before submission. Authorship and affiliations: To be supplied by the submitting authors. Research ethics: This conceptual study contains no human-participant or animal research.

REFERENCES

1. Borja, C., & Romeu, J. (2003). On the behavior of Koch island fractal boundary microstrip patch antenna. IEEE Transactions on Antennas and Propagation, 51(6), 1281–1291. https://doi.org/10.1109/TAP.2003.811479
2. Deb, K., Pratap, A., Agarwal, S., & Meyarivan, T. (2002). A fast and elitist multiobjective genetic algorithm: NSGA-II. IEEE Transactions on Evolutionary Computation, 6(2), 182–197. https://doi.org/10.1109/4235.996017
3. European Telecommunications Standards Institute. (2026). 5G; NR; User Equipment (UE) radio transmission and reception; Part 1: Range 1 Standalone (ETSI TS 138 101-1 V18.12.0). https://www.etsi.org/deliver/etsi_ts/138100_138199/13810101/18.12.00_60/ts_13810101v181200p.pdf
4. International Telecommunication Union. (2023). Framework and overall objectives of the future development of IMT for 2030 and beyond (Recommendation ITU-R M.2160-0). https://www.itu.int/rec/R-REC-M.2160-0-202311-I/en
5. Puente-Baliarda, C., Romeu, J., & Cardama, A. (2000). The Koch monopole: A small fractal antenna. IEEE Transactions on Antennas and Propagation, 48(11), 1773–1781. https://doi.org/10.1109/8.900236
6. Puente-Baliarda, C., Romeu, J., Pous, R., & Cardama, A. (1998). On the behavior of the Sierpinski multiband fractal antenna. IEEE Transactions on Antennas and Propagation, 46(4), 517–524. https://doi.org/10.1109/8.664115
7. Romeu, J., & Soler, J. (2001). Generalized Sierpinski fractal multiband antenna. IEEE Transactions on Antennas and Propagation, 49(8), 1237–1239. https://doi.org/10.1109/8.943320
8. Werner, D. H., & Ganguly, S. (2003). An overview of fractal antenna engineering research. IEEE Antennas and Propagation Magazine, 45(1), 38–57. https://doi.org/10.1109/MAP.2003.1189650
9. Yaminisasi, G., Pardhasaradhi, P., Reddy, S. S. M., Kumari, K. A., Kumar, O. P., Bhiradi, I., & Madhav, B. T. P. (2025). Optimization of compact fractal monopole antenna with partial fractal ground using machine learning approach for multiband applications. Scientific Reports, 15, Article 41999. https://doi.org/10.1038/s41598-025-26143-5